Optical Engineering

SPIEDigitalLibrary.org/oe

Laser-phased-array beam steering controlled by lithium niobate waveguides

Dengcai Yang
Zuoyun Yang
Dayong Wang

SPIE

Laser-phased-array beam steering controlled by lithium niobate waveguides

Dengcai Yang
Zuoyun Yang
Dayong Wang
Beijing University of Technology
Institute of Information Photonics Technology
Beijing 100124, China
and
Beijing University of Technology
College of Applied Science
Beijing 100124, China
E-mail: wdyong@bjut.edu.cn

Abstract. A laser steering system based on the Ti-diffusion lithium niobate ($LiNbO_3$) waveguides is presented. A phase shifter based on the $LiNbO_3$ waveguide is designed. This waveguide can provide a continuous phase shift for laser-phased-array (LPA) by changing the voltage loaded on it. The theory of irregular LPA based on the Ti-diffusion $LiNbO_3$ waveguide phase shifter is studied numerically and experimentally. Beam steering with an angle of 1.37 deg is gained by a 1×3 array setup that agrees well with the theory. [DOI: 10.1117/1.OE.53.6.061605]

Subject terms: laser-phased-array; electro-optic effect; lithium niobate; beam steering.

Paper 130977SS received Jul. 5, 2013; revised manuscript received Aug. 27, 2013; accepted for publication Aug. 29, 2013; published online Dec. 2, 2013.

1 Introduction

Laser-phased-array (LPA) technology has attracted many researchers for its potential application in both commercial and military fields for several decades. As an optical-phased–array,[1] LPA can inherently support beam steering at a high precision (sub-microradian) and resolution (tens of thousands of Rayleigh spots per dimension),[2] by controlling the phase of each array element.

Much progress for the LPA has been achieved around the world to obtain a good performance for scanning beam in recent years, including larger scanning angles and higher powers. Meanwhile, some LPA systems based on fiber,[3] waveguide,[4] Lanthanum-modified Lead Zirconate-Titanate,[5] and liquid crystal[6] were provided theoretically. However, it is difficult to obtain a good performance practically because the performance of the LPA system is affected by many factors. For example, some of the problem factors are pump beam quality, phase accuracy, polarization, distance between adjacent coherence beams, and impacts produced by the temperature variation and vibration. It is most necessary for precise and rapid phase controlling to improve the performance.

In this article, the lithium niobate ($LiNbO_3$) waveguide is designed to control the phase in the LPA system for its well electro-optic effect, quick response speed, and precise control of phase. Additionally, simulation for the LPA based on the $LiNbO_3$ waveguides is provided numerically, and an LPA system for 1×3 fiber LPA is established experimentally.

2 Theory

2.1 *Principal of Ti-Diffusion $LiNbO_3$ Waveguide Phase Shifter*

It is known that the $LiNbO_3$ crystal exhibits well electro-optical effect while loading the voltage on it. According to this, some properties of a light propagating in the crystal can be controlled, such as the phase, amplitude, and polarization, by changing the voltage. In this LPA system, the phase shifter is used. First, the appropriate waveguide structure should be designed on the crystal to restrict the propagation of the light. The titanium-diffused optical waveguide in $LiNbO_3$ is considerable since the diffused waveguide is electro-optically active and tight optical confinement is obtained with a low transmission loss.[7] The process of the Ti-diffusion $LiNbO_3$ waveguide is shown in Fig. 1. It is noted that the $LiNbO_3$ crystal should be Y-cut to take advantage of its biggest electro-optical coefficient of γ_{33}, which will be discussed. Second, channel waveguide along the X direction can be obtained from Ti-diffusion at a high temperature of 1050°C for 6.5 h, the width and the thickness of the initial Ti-strip are 5 μm and 110 nm, respectively, to ensure single mode propagation, which can effectively reduce the transmission loss and improve coupling efficiency with the fiber.[8] Finally, electrodes are added on both sides of the waveguide.

Additionally, a lower half-wave voltage is always desired for the LPA system. According to the electro-optical effect of the $LiNbO_3$ crystal, when the electric field is loaded along the Z direction, the variation of refractive index for the light with a polarization alone the Z direction is

$$\Delta n_e = -\frac{1}{2} n_e^3 \gamma_{33} E_Z, \tag{1}$$

where n_e is the refractive index of extraordinary light in $LiNbO_3$ crystal, γ_{33} is the biggest electro-optical coefficient of the $LiNbO_3$ crystal, and E_Z is the electric field loaded along the Z direction. Then, it is easy to obtain the variation of the phase. Supposing L is the length of the electric field and d is the space between two electrodes

$$\Delta\varphi = \frac{2\pi}{\lambda} \times \Delta n_e \Gamma \times L = \frac{\pi}{\lambda} n_e^3 \gamma_{33} E L \Gamma = \frac{\pi V}{\lambda d} n_e^3 \gamma_{33} L \Gamma, \tag{2}$$

where $V = E \times d$, λ is the wavelength of the light source, the Γ is the overlap integral between the applied electric field and the optical mode,[9] which cannot be ignored in the real case. The half-wave voltage is always defined as

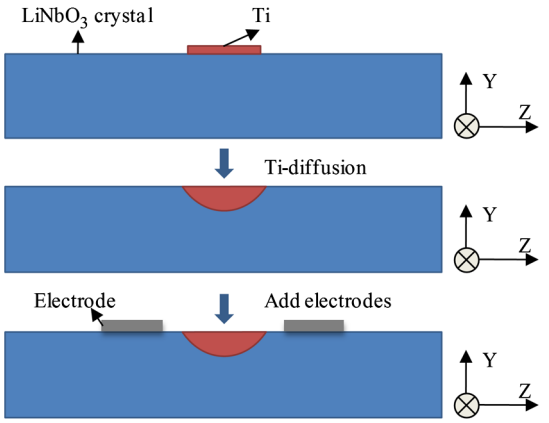

Fig. 1 Principal diagram of Ti-diffusion.

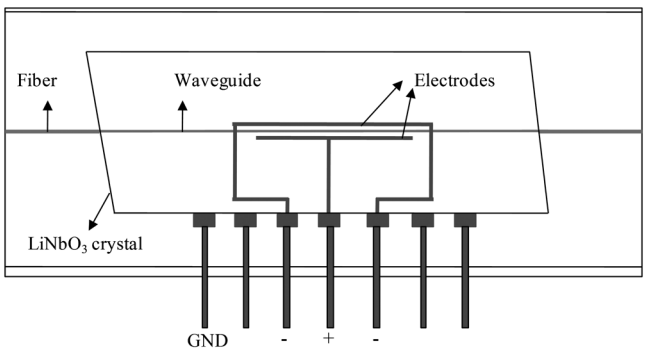

Fig. 2 Structure of the Ti-diffusion $LiNbO_3$ waveguide phase shifter.

$$V_\pi = \frac{\lambda d}{n_e^3 \gamma_{33} L \Gamma}. \tag{3}$$

Lower half-wave voltage can be achieved through designing appropriate values of d and L. According to the current processing level, suppose that the L is equal to 1.5 cm and d is equal to 11 μm. Considering the $\gamma_{33} = 30.8 \times 10^{-12}$ m/V and $n_e = 2.1373$, $\Gamma = 0.5$,[10,11] a lower half-wave voltage of 5.2 V is obtained numerically according to Eq. (3). Substituting Eqs. (3) into (2).

$$\Delta\varphi = \frac{\pi V}{V_\pi}. \tag{4}$$

Based on the above theory, the structure of the Ti-diffusion $LiNbO_3$ waveguide phase shifter is designed, as shown in Fig. 2.

Simulations are performed with the commercial software BeamProp (RSoft) to obtain a good performance of the phase shifter. The electric potential produced by the electrodes and the optical intensity through the propagation has been simulated, as shown in Fig. 3. This waveguide phase shifter has a low transmission loss and the electric field can be added effectively. (The axes X, Y, and Z in simulation are corresponding to the axes Z, Y, and X in the actual $LiNbO_3$ crystal.)

2.2 *Theoretical Model of LPA*

The two-dimensional array, including large number of emitters, is desired to gain high power, high resolution, and a big steering angle. In this experiment, the one-dimensional (1-D) array is considered. The radiation pattern of a 1-D array of emitters in far field is always calculated using the Fraunhofer approximation.[12] The amplitude of the far-field pattern is written as

$$U_{\text{array}}(x, y) = C \int A(x, y) \times \exp(-ikx \sin\theta_x) \mathrm{d}x, \tag{5}$$

where C is a constant, $A(x, y)$ is the amplitude of the entire emitting array as a function of position (x, y), $k = 2\pi/\lambda$, and $\sin\theta_x = x/z$, where z is the propagation distance of the coherent beam along the Z direction. It is assumed that the beam is identical with a Gaussian amplitude distribution, so the amplitude $A(x, y)$ can be written as

$$A(x, y) = \sum_{m=1}^{N_x} A_m \exp\left[-\left(\frac{x^2 + y^2}{w_0^2}\right) + i\varphi_m\right] \times \delta[x - md], \tag{6}$$

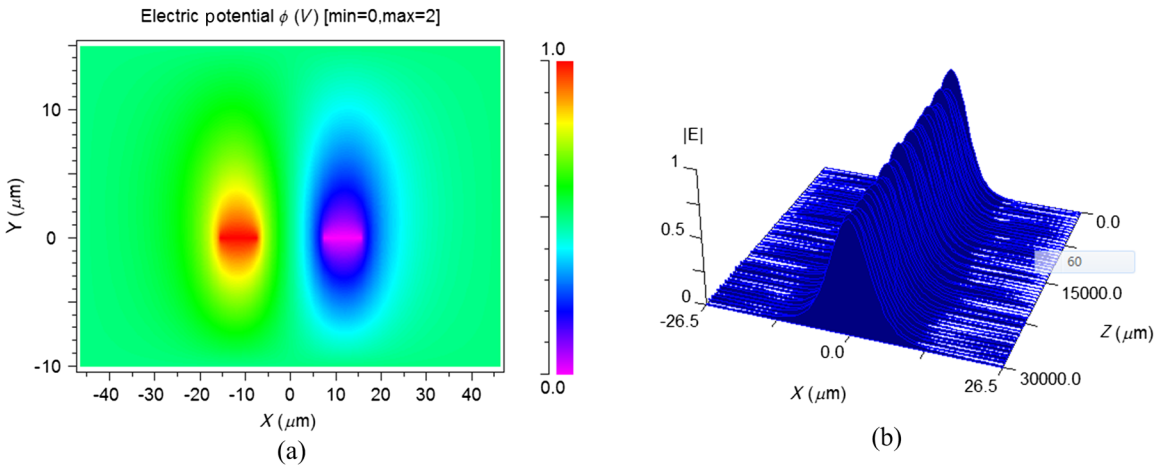

Fig. 3 (a) The electric potential and (b) optical intensity field in the Ti-diffusion $LiNbO_3$ waveguide.

where N_x is the number of emitters in the array, m corresponds to the position of each element, which ranges from 1 to N_x, d is the space between adjacent elements, ω_0 is the radius of Gauss beam waist, and φ_m is the phase of the Gauss beam. Considering the convolution theorem, Eq. (6) is substituted into Eq. (5), and the following can be obtained

$$I(\theta_x,\theta_y) \propto \left|\sum_{m=1}^{N_x} A_m \exp[-i(kmd\theta_x+\varphi_m)]\right|^2 \times \exp\left[-\frac{1}{2}k^2\omega_0^2(\theta_x^2+\theta_y^2)\right], \quad (7)$$

where θ_x and θ_y are the angles of point (x,y) in the x and y directions correspondingly, and can be approximated at x/z and y/z, respectively. The first term on the right-hand side is the factor determined by the array configuration and the second term is the form factor determined by the properties of the emitters themselves. Therefore, the intensity pattern in the far field should have such show a characteristic as one central string with sidelobes. While the phase shift between adjacent elements is changed, the position of the central string will move correspondingly. Therefore, beam steering can be obtained by changing the phase shift between adjacent elements in the array.

However, the sidelobes that can affect the scanning accuracy are undesirable, and d should be less than the wavelength in the regular array to suppress the sidelobes. It is actually difficult to achieve. Fortunately, the irregular array was researched, which indicates that the suppression of sidelobes can be achieved to some extent if the inter-element space is irregular.[13] Then, Eq. (7) can be rewritten as

$$I(\theta_x,\theta_y) \propto \left|\sum_{m=1}^{N_x} A_m \exp[-i(kd_m\theta_x+\varphi_m)]\right|^2 \times \exp\left[-\frac{1}{2}k^2w_0^2(\theta_x^2+\theta_y^2)\right], \quad (8)$$

where d_m is the position of the m'th element.

Assuming that the phase offset between adjacent elements is $\Delta\varphi$ and considering Eq. (4), the intensity is obtained by

$$I(\theta_x,\theta_y) \propto \left|\sum_{m=1}^{N_x} A_m \exp\left[-i\left(kd_m\theta_x+\frac{\pi V_m}{V_\pi}\right)\right]\right|^2 \times \exp\left[-\frac{1}{2}k^2w_0^2(\theta_x^2+\theta_y^2)\right], \quad (9)$$

where V_m is the applying voltage on the m'th element and its value should correspond to d_m.

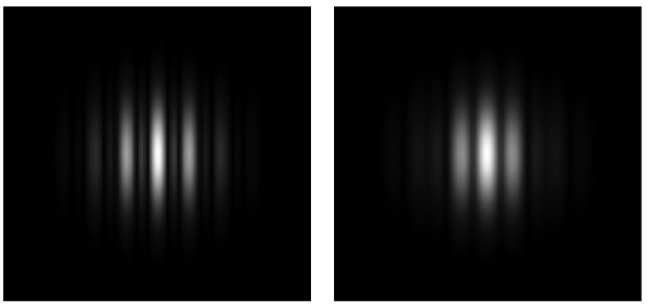

(a) (b)

Fig. 4 Intensity distribution of (a) regular array for $\Delta d_1 = \Delta d_2 = 250\ \mu$m and (b) irregular array for $\Delta d_1 = 250\ \mu$m, $\Delta d_2 = 300\ \mu$m. (Δd_1 and Δd_2 are the space between adjacent elements.)

3 Numerical Simulation

The intensity distribution of 1×3 LPA in the far field is simulated numerically to verify the theoretical analysis. First, the simulation of a regular array and an irregular array without phase shift are shown in Fig. 4. It shows that the irregular array can suppress the sidelobes to a certain extent. Then, V_m has been changed to simulate the result of beam steering in the irregular array, as shown in Fig. 5. For all the simulations, it is supposed that $\omega_0 = 3\ \mu$m, $\lambda = 1.06\ \mu$m, $V_\pi = 5$ V, and $z = 10$ m, according to the experimental conditions.

4 Experiment

4.1 *Introduction of Experimental Setup*

The experimental setup diagram is shown in Fig. 6. The laser source, with a wavelength of 1060 nm, is divided into three channels using two Y-branch power splitters. One is regarded as the reference beam and the other two beams whose phases can be independently controlled by the $LiNbO_3$ waveguide

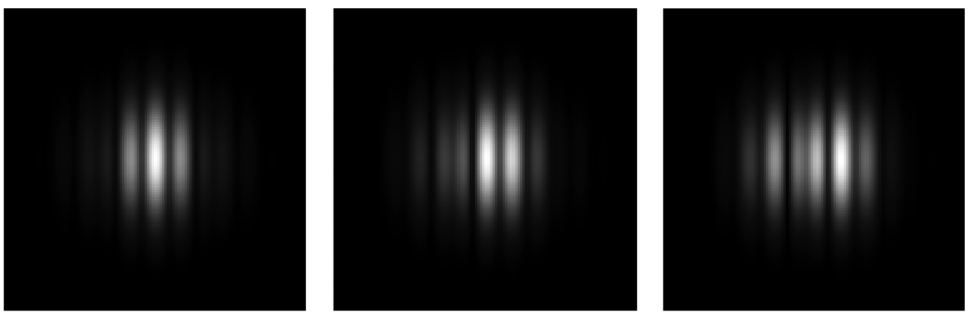

(a) (b) (c)

Fig. 5 The beam steering of the irregular array for $\Delta d_1 = 250\ \mu$m and $\Delta d_2 = 300\ \mu$m. (a) $V_1 = V_2 = V_3 = 0$ V and (b) $V_1 = 0$ V, $V_2 = 1$ V, and $V_3 = 2.2$ V, (c) $V_1 = 0$ V, $V_2 = 2$ V, and $V_3 = 4.4$ V. (Δd_1 and Δd_2 are the space between adjacent elements.)

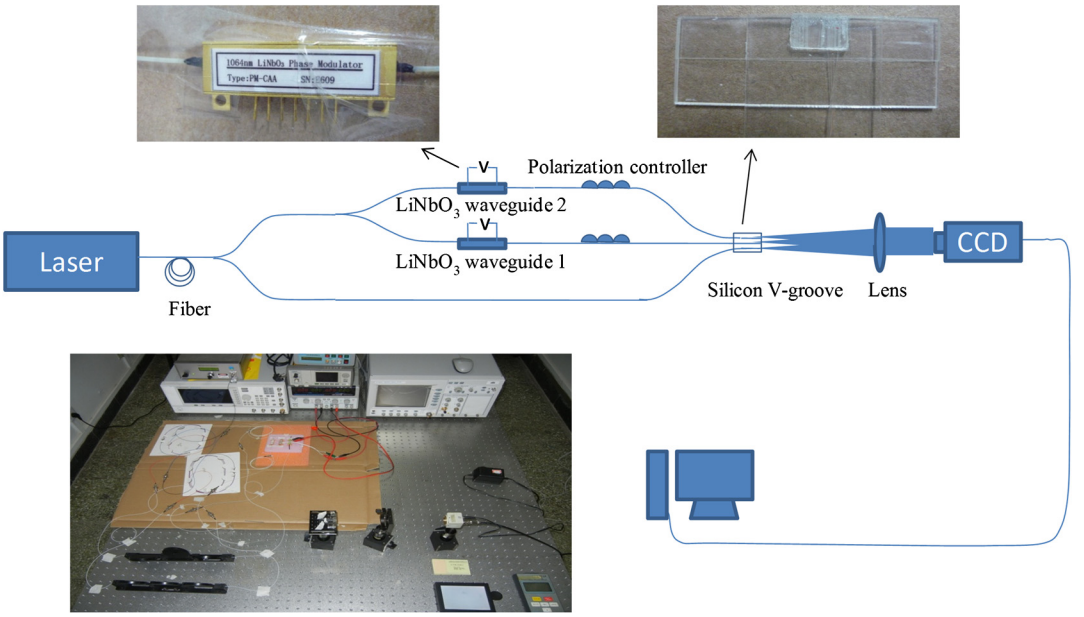

Fig. 6 Schematic diagram of the 1×3 fiber laser-phased-array system.

phase shifter that has a low half-wave voltage of 5 V. The polarization of each beam should be adjusted to be consistent with the $LiNbO_3$ waveguide. The three output beams are assembled on a silicon V-grove for beam coherence in space. The inter-element spaces are 250 μm and 300 μm. An infrared image detector (CCD) is used to observe the intensity distribution in the far field at the focal plane of a lens with the focal length of 150 mm. All the fibers used in the experiment are single mode fibers with the core diameter of 6 μm.

4.2 *Experimental Results and Discussion*

In this experiment, the power of the laser source was <1 mW to observe the pattern from the CCD clearly. First, there is no voltage loaded on both the $LiNbO_3$ waveguide phase shifters, therefore the pattern with a central string and sidelobes can be obtained from the CCD as shown in Fig. 7(a). Then, the voltage loaded on the $LiNbO_3$ waveguide 1 and $LiNbO_3$ waveguide 2 was 1 and 2.2 V, respectively. Figure 7(b) shows that the central string moves a distance toward one direction. What is more, Fig. 7(c) shows that the central

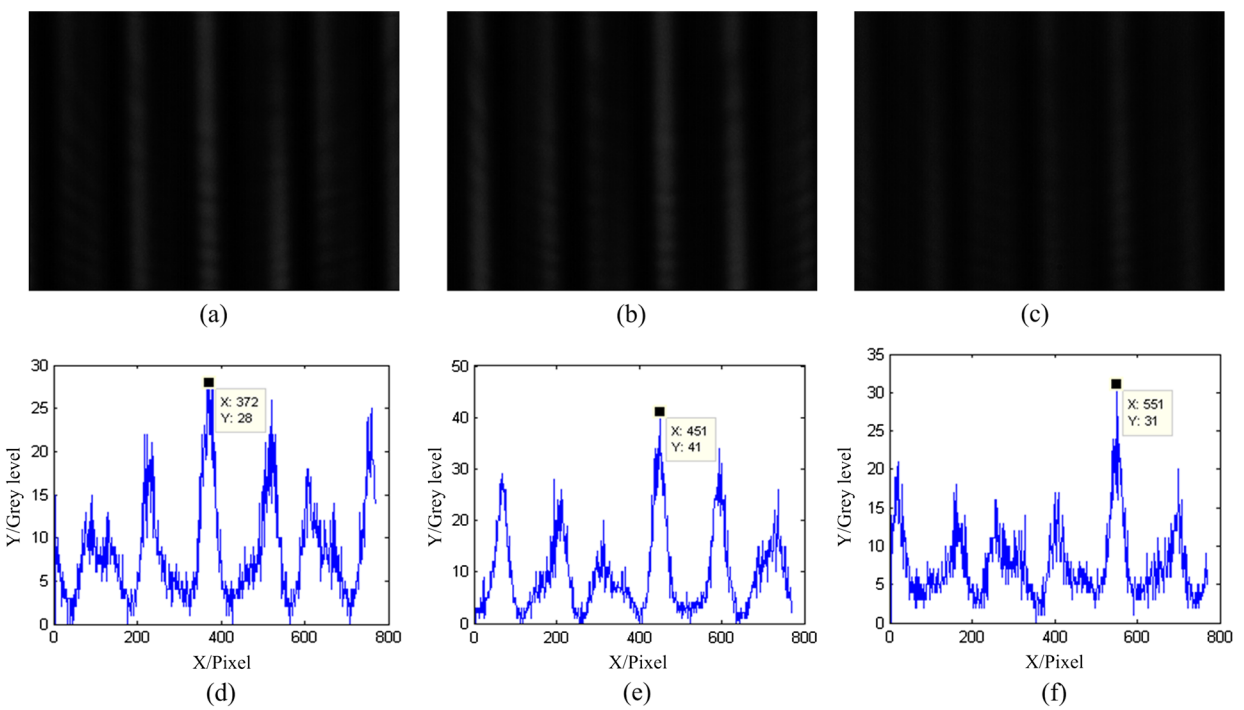

Fig. 7 The experimental results when loading different voltages: (a) $V_1 = V_2 = V_3 = 0$ V, (b) $V_1 = 0$ V, $V_2 = 1$ V, and $V_3 = 2.2$ V, (c) $V_1 = 0$ V, $V_2 = 2$ V, and $V_3 = 4.4$ V, and the cross-sections, (d) the cross-section of (a), (e) the cross-section of (b), (f) the cross-section of (c).

string travels the larger distance when the voltage increased to 2 and 4.4 V, respectively, which agrees with the numerical simulation. However, the larger the shift distance, the more the sidelobes increase, which spreads the energy of the main lobe and significantly affects the scanning accuracy.

The beam shift angle θ was defined to describe the system performance

$$\sin\theta = \Delta x/f, \tag{10}$$

where Δx is the shift distance of the central string, and f is the focal length of lens in the system. The cross-section of each pattern was taken to observe the shift distance of the central string, as shown in Figs. 7(d)–7(f) and the position of the central string was also provided in each figure. Considering the CCD used in the experiment with the pixel pitch of 20 μm, the shift distance of 3.58 mm was gained in Fig. 7(f) comparing with Fig. 7(d). Accordingly, the beam shift angle of 1.37 deg was obtained for the system since the f is 150 mm.

5 Conclusions

The Ti-diffusion $LiNbO_3$ waveguide phase shifter was designed to control the phase of the inter-element in irregular LPA. The beam steering was achieved from both simulation and experiment by changing the voltage loaded on both the Ti-diffusion $LiNbO_3$ waveguide phase shifters. More array elements and smaller space between adjacent elements are necessary for a better LPA performance.

Acknowledgments

This work is financially supported by the National Natural Science Foundation of China (Nos. 61077004 and 61205010), Beijing Municipal Natural Science Foundation (No. 1122004), Science Foundation of Education Commission of Beijing (No. KZ200910005001), and Innovative Talent and Team Building Project for Serving Beijing.

References

1. R. A. Meyer, "Optical beam steering using a multichannel lithium tantalite crystal," *Appl. Opt.* **11**(3), 613–616 (1972).
2. T. A. Dorschner et al., "An optical phased array for lasers," in *IEEE Int. Symposium on Phased Array Systems and Technology*, Boston, MA, pp. 5–10 (1996).
3. D. C. Jones et al., "Beam steering of a fiber-bundle laser output using phased array techniques," *Proc. SPIE* **5335**, 125–131 (2004).
4. F. Vasey et al., "Spatial beam steering with an AlGaAs integrated waveguides," *Appl. Opt.* **32**(18), 3220–3232 (1993).
5. J. A. Thomas and Y. Fainman, "Optimal cascade operation of optical phased-array beam deflectors," *Appl. Opt.* **37**(26), 6196–6212 (1998).
6. T. A. Dorschner et al., "Electronic beam control for advanced laser radar," *Proc. SPIE* **3707**, 316–326 (1999).
7. W. K. Burns, P. H. Klein, and E. J. West, "Ti diffusion in Ti:$LiNbO_3$ planar and channel optical waveguides," *J. Appl. Phys.* **50**(10), 6176–6182 (1979).
8. M. A. R. Franco, L. C. Vasconcellos, and J. M. Machado, "Coupling efficiency between optical fiber and Ti:$LiNbO_3$ channel waveguide," *Telecommunications* **7**(1), 54–59 (2004).
9. R. C. Alferness, "Waveguide electro-optic modulators," *IEEE Trans. Microwave Theory Tech.* **MTT-30**(8), 1121–1137 (1982).
10. C. M. Kim and R. V. Ramaswamy, "Overlap integral factors in integrated optic modulators and switches," *J. Lightwave Technol.* **7**(7), 1063–1070 (1989).
11. D. Janner et al., "Micro-structured integrated electro-optic $LiNbO_3$ modulators," *Laser Photon. Rev.* **3**(3), 301–313 (2009).
12. M. Born and E. Wolf, *Principles of Optics*, pp. 386–387, Pergamon Press, New York (1980).
13. J. H. Abeles and R. J. Deri, "Suppression of sidelobes in the far field radiation patterns of optical waveguide arrays," *Appl. Phys. Lett.* **53**(15), 1375–1377 (1988).

Dengcai Yang received his BS and MSc degrees in optoelectronics in 2001 and 2006 from Beijing Institute of Technology, China. Now, he is a PhD candidate in optical engineering in the Beijing University of Technology. His main research interests are laser coherence.

Zuoyun Yang received his BS degrees in applied physics in 2008 from Shenyang University of Technology, China. Now, he is studying for a master's degree in the Beijing University of Technology. His main research interests are optical communication and optical information processing.

Dayong Wang received his BS degree in optical engineering in 1989 from Huazhong University of Science and Technology, Wuhan, China, and his PhD degree in physics in 1994 from Xi'an Institute of Optics and Fine mechanics, Chinese Academy of Sciences. From 1994 to 1996, he worked as a post-doctoral in Xidian University, China. In 1996, he joined the Department of Applied Physics, Beijing University of Technology (BJUT). From 1998 to 2000, he worked in the Weizmann Institute of Science, Israel, as a visiting scientist. Since 2000, he has been a professor in the College of Applied Sciences, BJUT. His research interests include optical information processing, optical storage, holography, and diffractive optical elements. He is a member of COS, SPIE, and OSA.